

DR2005068

GSA Data Repository Items

Figure DR1. Vibra- and piston-cores collected at Cave Rock (a & b) and on the hanging-wall of the Stateline fault (c) are shown. The location of OSL and carbon samples is shown for vibra- and piston-cores, including estimated dates and errors. OSL samples (b) were analyzed at three locations above or near the cobble layer at 5.5, 6.1 and 6.5 m. Although all three locations returned age estimates less than 16.6 ka, only the sample at 5.5 m (16.6 ka) provided enough aliquots (42) to establish an error estimate (± 1.8 ka). Extrapolation of the overlying sedimentation rate (between 0 and 5.5 m) gives an estimated age of 19.2 ka for the abrasion surface. An additional vibra-core (c) collected <100 m outboard of this clinoform contained minor amounts of datable carbon, revealing a compressed time section. For example, carbon found at 0.155 m was dated by the AMS (accelerator mass spectrometry) ^{14}C technique at 10.5 ± 0.04 ka, for an extrapolated estimate of 17.3 ka for the paleosurface. This simple estimate should be treated with some caution because the three dated samples suggest an incomplete sedimentation record. Nevertheless, these samples indicate an age for the surface that is consistent with nearby OSL results. Inset (d) shows AMS ^{14}C dates versus depth, highlighting an early- to mid-Holocene sedimentation rate of 0.4 mm/yr. Sample collected in turbidites are biased toward older ages, consistent with older material being transported down-slope.

Figure DR2. A number of other lines of evidence can be used to corroborate a lowstand of lake level. CHIRP profiles collected in the shallow waters in front of the Tahoe City

dam, the location of the lake's natural sill, reveal an in-filled channel that is approximately 13 m in depth with truncation along the southern channel wall, indicating channel incision and down-cutting. A sample CHIRP profile (a) of the paleo-channel near Tahoe City is shown. Note the truncated lake sediments (left) and the strong reflection from the channel wall (right). The red line in the sub-diagram (b) reveals our best interpretation of the channel boundary (13 m maximum depth). The channel was likely cut after younger Tahoe glaciation, which lowered the lake level to some 13 m beneath the present level; erosion and truncation occurred during this period until the abrasion surface was flooded near the last glacial maximum, during Tioga glaciation 20 ka before present. The subsequent raising of lake level after in-filling of the channel, has minimized any recent down-cutting of footwall strata.

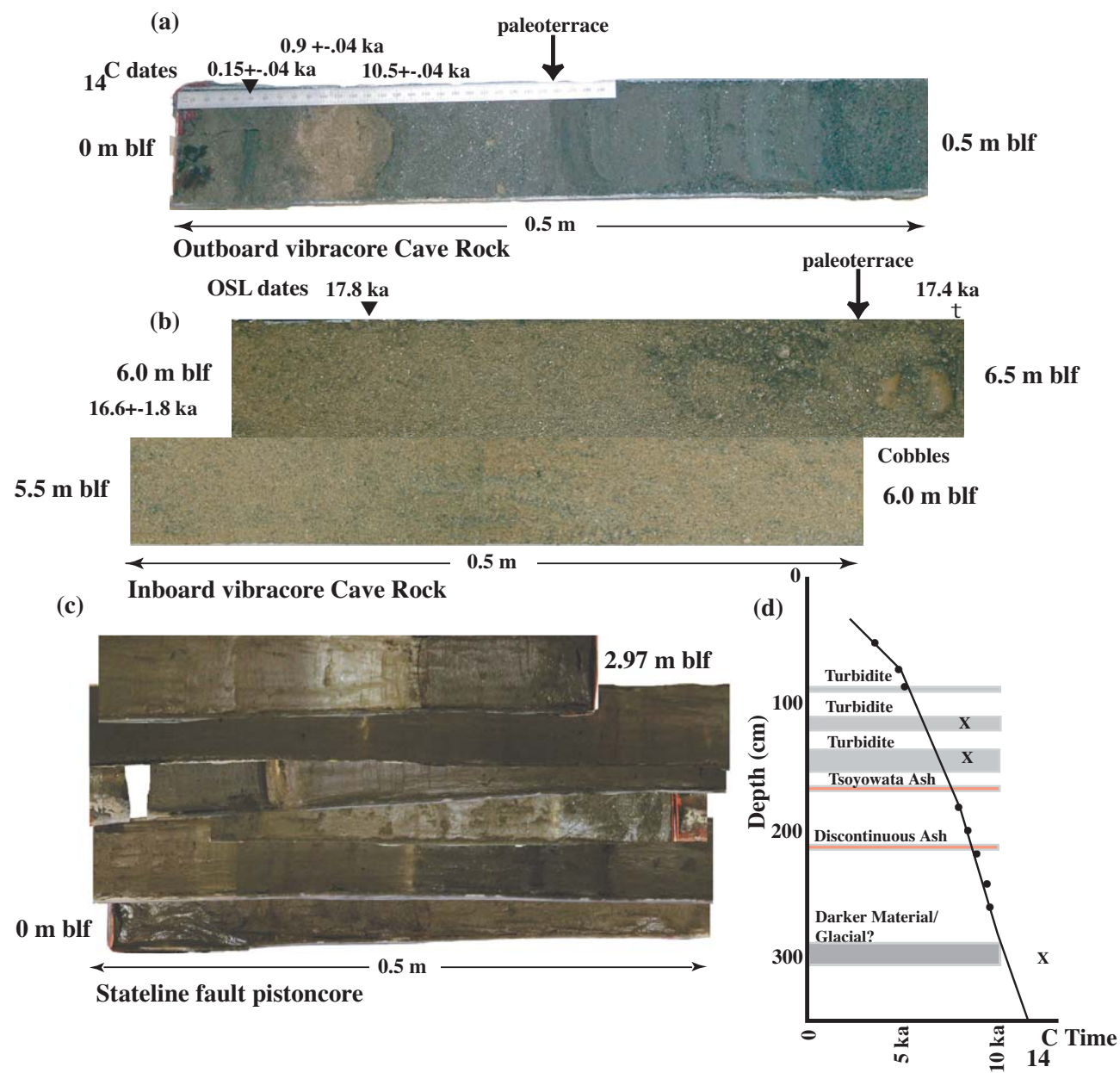


Figure DR1

(a)

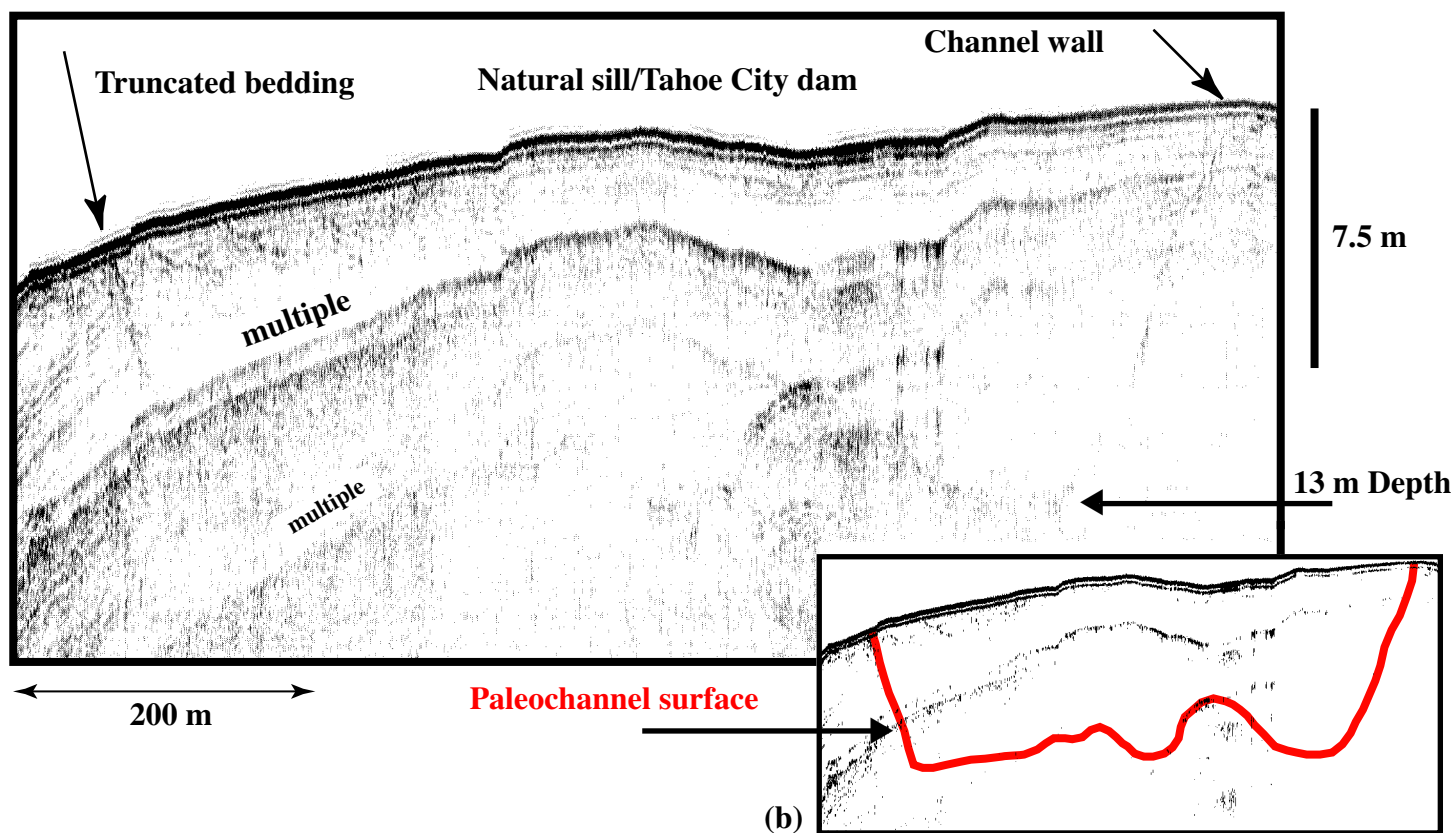


Figure DR2

Appendix DR1: Data and Methods

To place quantitative constraints on slip rates across several submerged faults in the Tahoe basin, sonar- and lidar-derived bathymetry were integrated with subbottom seismic CHIRP profiles to document vertical deformation across the West Tahoe, Stateline, and Incline Village normal faults. Marker beds were sampled either directly with sediment cores or indirectly by using an extrapolation of sedimentation rate, to establish age constraints on these surfaces.

For water depths of >20 m, bathymetric data were collected by using standard multibeam sonar techniques. This data set was acquired in summer 1998 through the use of a SIMRAD EM 1000 swath-mapping system (Gardner et al., 2000). To bridge the gap between existing shoreline and multibeam data sets, the shallow shelves (<20 m) encircling Lake Tahoe were mapped in 2000 by using the U.S. Army Corps of Engineers SHOALS airborne laser bathymetry system. Images of subsurface structure were collected between 1999 and 2004 by using an EdgeTech SUBSCAN CHIRP profiler. This seismic profiler transmits a frequency-modulated pulse that linearly sweeps over a frequency range between 1 and 6 kHz, enabling resolution between subbottom layers down to tens of centimeters. In practice, the resolution of most of the SUBSCAN records beneath Lake Tahoe was ~0.5 m in shallow locales and ~1 m for deeper records.

Appendix DR1 References Cited

Gardner, J.V., Mayer, L.A., and Hughs Clarke, J.E., 2000, Morphology and processes in Lake Tahoe (California–Nevada): Geological Society of America Bulletin, v. 112, p. 736–746.

Appendix DR2: Optically Stimulated Luminescence Dating

Introduction

Optically stimulated luminescence (OSL) dating is used to determine the time elapsed since a sediment sample was exposed to daylight. This technique has been successfully applied to dating deformed sediments for paleoseismic studies in the western USA (e.g. Machette *et al.*, 1992; Crone *et al.*, 1997; Rockwell *et al.*, 2000; Lee *et al.*, 2001;) and elsewhere in the world (e.g. Owen *et al.*, 1999; Washburn *et al.*, 2001). The technique relies on the interaction of ionizing radiation with electrons within semi-conducting minerals resulting in the accumulation of charge in metastable location within minerals. Illuminating the minerals and detrapping the charge that combines at luminescence centers can determine the population of this charge. This results in the emission of photons (luminescence). Artificially dosing sub-samples and comparing the luminescence emitted with the natural luminescence can determine the relationship between radiation flux and luminescence. The equivalent dose (D_E) experienced by the grains during burial therefore can be determined. The other quantity needed to calculate the age is the ionizing radiation dose rate, which can be derived from direct measurements or measured concentrations of radioisotopes. The age is then derived using the equation:

$$\text{Age} = D_E / \text{dose rate}$$

The uncertainty in the age is influenced by the systematic and random errors in the D_E values and the possible temporal changes in the radiation flux. The quoted error is the deviation of the D_E values on multiple sub-samples and the error in measured ionizing

radiation dose rate or the concentration of radioisotopes. It is not possible to determine temporal changes in the dose rate that is a consequence of changes in water content and the growth and/or translocation of minerals within the sediment. The dose rate is therefore generally assumed to have remained constant over time.

Methods and Technical Details

The OSL measurements were undertaken at the Luminescence Dating Laboratory at the University of California, Riverside. The *in situ* water content (mass of moisture/dry mass; Aitken, 1998) was determined using sub-samples by drying them in an oven at 50°C. The sample for dating was dry sieved to obtain a 90-125 µm or a 125-180 µm particle size fraction. The carbonates and organic matter were removed from the 90-125 µm or the 125-180 µm fraction using 10% HCl and 30% H₂O₂, respectively. Sodium polytungstate solutions of different densities and a centrifuge were used to separate the quartz and feldspar-rich fractions from the heavy minerals. The separated quartz-rich fraction was treated with 49% HF for 80 minutes to dissolve any plagioclase feldspars and remove the alpha-irradiated surface of the quartz grains. Dried quartz grains were mounted on stainless steel discs with silicon spray. All the preparation techniques were carried out under laboratory safelights to avoid sample bleaching.

Approximately 20 g of the dried sub-sample from the sediment sample was ground to a fine powder and sent to the Becquerel Laboratories at Lucas Heights in Australia for INAA. Using dose-rate conversion factors of Adamiec and Aitken (1998) and beta attenuation factors of Mejdahl (1979) and Adamiec and Aitken (1998), the elemental

concentrations were converted into external beta and gamma components, which were in turn attenuated for moisture content. These were summed together with a cosmic ray component using the methods of Prescott and Hutton (1994) to give estimates of the total dose-rate for each sample (Table 1). Variable water content throughout the section may have occurred throughout the history of the section. However, it is not possible to determine the degree of such changes and we have assumed that the dose rate has remained constant, but have used $10 \pm 5\%$ water content to help account for possible changes in water content.

Luminescence measurements were undertaken using a Daybreak 1100 automated system with an 1100FO/L combined fiber-optic/IRLED illuminator for optical stimulation (Bortolot, 1997). Luminescence from the quartz grains was stimulated using a 150 W halogen lamp producing green light (514 ± 34 nm; $\sim 20 \text{ mWcm}^{-2}$) defined by an additional narrow band interference filter. All quartz samples were screened for feldspar contamination using infrared stimulation from T-1 GaAlAs diodes (880 ± 80 nm; diode current 20 mA). All OSL signals were detected with a photomultiplier tube characterized by 9 mm Schott UG11 ultraviolet detection filters. Daybreak TLApplic 4.30 software was used for hardware control and DE analysis.

D_E measurements were determined on multiple aliquots for each sample using the SAR protocol developed by Murray and Wintle (2000). In the SAR method, each natural or regenerated OSL signal is corrected for changes in sensitivity using the OSL response to a subsequent test dose. The natural dose (N) was measured in the first cycle, and

thereafter five regeneration doses (R₁ to R₅) were administered. The first three were used to bracket the natural luminescence level ($R_1 < N \sim R_2 < R_3$), the fourth (R₄) was set at zero to monitor recuperation (i.e. R₄/N) and to monitor the reproducibility of sensitivity corrections the fifth dose was made that had an equal to the first dose (i.e. R₅/R₁). Each measurement cycle comprised a regeneration dose (zero for natural), preheating of 220°C for 10 s, optical stimulation for 100 s (sample temperature of 125°C), a constant test-dose, a test-preheat of 160°C for 0 s and a final optical stimulation for 100 s (at 125°C). The net-natural and net-regenerated OSL were derived by taking the initial OSL signal (0-1 s) and subtracting a background from the last part of the stimulation curve (90-100 s); subtracting the background from the preceding natural and regenerative OSL signals derived the net test-dose response. Growth curves were plotted using the net natural and regenerated data divided by the subsequent response to the net-test dose. The growth curve data was fitted with either a single saturating exponential. The D_E for each sample was calculated using the mean values and standard error of all the aliquots for each sample (Table 1). The INAA, cosmic dose rates, total doses, mean D_E and OSL ages are shown in Table 1.

Appendix DR2 References Cited

Adamiec, G., and Aitken, M., 1998. Dose-rate conversion factors: update: *Ancient TL*, 16, 37-50.

Aitken, M.J., 1998. *An introduction to optical dating*. Oxford University Press, Oxford.

Bortolot, V.J., 1997. Improved OSL excitation with fiberoptics and focused lamps. *Radiation Measurements*, 27, 101-106.

Crone, A.J., Machette, M.N., Bradley, L-A. and Mahan, S.A. 1997. Late Quaternary surface faulting on the Cheraw Fault, Southeastern Colorado. *Geologic Investigations*

Map, USGS Map I-2591.

Lee, J., Spencer, J.Q. and Owen, L.A., 2001. Holocene slip rates along the Owens Valley fault, California: implications for the recent evolution of the Eastern California Shear Zone. *Geology*, 29, 819–822.

Machette, M.N., Personius, S.F. and Nelson, A.R., 1992. The Wasatch Fault Zone, USA. *Annales Tectonicae*, 6, 5-39, 5-39.

Mejdahl, V., 1979. Thermoluminescence dating: Beta attenuation in quartz grains. *Archaeometry*, 21, 61-73.

Murray, A. S., and Wintle, A. G., 2000. Luminescence dating of quartz using an improved single-aliquot regenerative-dose protocol. *Radiation Measurements*, 32, 57-73.

Owen, L.A., Cunningham, W.D., Richards, B., Rhodes, E.J., Windley, B.F., Dornjamjaa, D., Badamgarav, J., 1999. Timing of formation of forebergs in the northeastern Gobi Altai, Mongolia: implications for estimating mountain uplift rates and earthquake recurrence intervals. *Journal of the Geological Society*, 156, 3, 457-464. Erratum: *Journal of the Geological Society*, 156, Contents xii.

Prescott, J. R., and Hutton, J. T., 1994. Cosmic ray contributions to dose rates for luminescence and ESR dating: Large depths and long-term time variations. *Radiation Measurements*, 23, 497-500.

Prescott, J. R., and Stephans, L. G., 1982. Contribution of cosmic radiation to environmental dose. *PACT*, 6, 17-25.

Rockwell, T.K., Lindvall, S., Herzberg, M., Murbach, D., Dawsaon, T. and Berger, G., 2000. Paleoseismology of the Johnson Valley, Kicjapoo, and Homestead Valley Faults: clustering of earthquakes in the Eastern California Shear Zone. *Bulletin of the Seismological Society of America*, 90, 5, 1200-1236.

Washburn, Z., Arrowsmith, J.R., Forman, S.L., Cowgill, E., Wang Xiaofeng, Zhang Yueqiao and Chen Zhengle, 2001. Late Holocene earthquake history of the central Altyn Tagh fault, China. *Geology*, 29, 11, 1051-1054.

Zimmerman, D. W., 1971. Thermoluminescence dating using fine grains from pottery. *Archaeometry*, 13, 29-52.

Table DR1. Summary of OSL dating results from quartz extracted from sediment matrices: sample locations, radioisotope concentrations, moisture contents, total dose-rates, D_e estimates and optical ages

Sample #	Particle size (μm)	Location (N, E)	a.s.l. (m)	Depth (cm)	U ^a (ppm)	Th ^a (ppm)	K ^a (%)	Rb ^a (ppm)	W _{in-situ} ^b (%)	Cosmic ^c (mGya ⁻¹)	Dose-rate ^d (mGya ⁻¹)	n ^e	N ^f	Mean D _e ^g (Gy)	Age (ka)
265	125-180	35°, 120°	1899	610	8.33	34.8	2.4	89.0	10	0.075	5.82±0.35	25	6	74.3±21.0	12.8±1.8
266	125-180	35°, 120°	1899	650	9.47	36.1	2.5	94.5	10	0.073	6.21±0.37	9	3	92.0±24.8	14.8±2.6
267	90-125	35°, 120°	1899	547	8.80	33.6	2.2	98.4	10	0.079	6.03±0.34	42	16	100.2±31.2	16.6±1.8

^aElemental concentrations from NAA of whole sediment measured at Becquerel Laboratories, Lucas Heights, NSW, Australia. Uncertainty taken as ±10%.

^bEstimated fractional water content from whole sediment (Aitken, 1998). Uncertainty taken as ±5%.

^cEstimated contribution to dose-rate from cosmic rays calculated according to Prescott and Hutton (1994). Uncertainty taken as ±10%.

^dTotal dose-rate from beta, gamma and cosmic components. Beta attenuation factors for U, Th and K compositions incorporating grain size factors from Mejdahl (1979). Beta attenuation factor for Rb arbitrarily taken as 0.75 (cf. Adamiec and Aitken, 1998). Factors utilized to convert elemental concentrations to beta and gamma dose-rates from Adamiec and Aitken (1998) and beta and gamma components attenuated for moisture content.

^eNumber of aliquots measured.

^fNumber of replicated D_e estimates used to calculate mean D_e. These are based on recuperation and mismatches of < 10%.

^gMean equivalent dose (D_e) determined from replicated single-aliquot regenerative-dose (SAR; Murray and Wintle, 2000) runs. Errors are 1-sigma standard errors (ie. $\sigma_{n-1}/n^{1/2}$) incorporating error from beta source estimated at about ±5%.